Electronic excitation and dissociation of O_2 and S_2 by electron impact

Bruce C. Garrett, Lynn T. Redmon, C. W. McCurdy,* and Michael J. Redmon
Chemical Dynamics Corporation, 1550 West Henderson Road, Columbus, Ohio 43220
(Received 26 December 1984)

The impact-parameter method is used to calculate integral cross sections for electronic excitation and dissociation of O_2 and S_2 by electron impact. For both molecules, excitations to bound and dissociative states are considered for transitions from the ground electronic state ($X\,^3\Sigma_g^-$) to the two lowest states of $^3\Sigma_u^-$ symmetry (labeled B and E for O_2 and B and 2 for S_2) and the lowest state of $^3\Pi_u$ symmetry. The dependence of the cross sections upon initial vibrational and rotational states is studied for low collision energies (threshold to 25 eV). For some transitions a change in initial vibrational state can have a significant effect upon the cross sections, but, in general, the effect of changing the initial rotational state is small.

I. INTRODUCTION

The electronic excitation and dissociation of O_2 in collisions with low-energy electrons is an important process in the photochemistry of the upper atmosphere and in some gas-discharge lasers. For example, in gas lasers dissociative excitation can significantly affect the efficiency of the laser. Although the spectroscopy of the oxygen molecule has been studied extensively,[1] there have been only a few experimental measurements of cross sections for electronic excitation by electron impact. Lawrence[2] and Mumma and Zipf[3] have measured electron-impact cross sections for dissociation through excited electronic states which are higher than 15 eV above the ground state. Linder and Schmidt[4] have measured integral cross sections for spin-forbidden transitions to bound vibrational states, and Trajmar *et al.*[5,6] have measured differential and integral cross sections for spin-forbidden transitions to bound vibrational states. More recently, Wakiya[7] has measured differential and integral cross sections for the X-to-B and some spin-forbidden transitions, and there has been one calculation by Chung and Lin[8] of the cross section for dissociation through the B state of O_2. In the present paper we are interested in optically allowed transitions to bound vibrational states and to dissociative states of low-lying electronic states which are accessible in collisions with low-energy electrons that are present in gas-discharge lasers.

The sulfur molecule is a possible candidate for a gas laser[9] and has been extensively studied spectroscopically,[10] but little is known about its cross sections for electron-impact excitation and dissociation. Because the O_2 and S_2 molecules are isoelectronic, it is interesting to compare the analogous electron-impact cross sections of these systems.

In this paper, electron-impact cross sections for optically allowed transitions of ground-state O_2 and S_2 to bound and dissociative states are presented. The cross sections are for conditions relevant to laser plasmas: initial relative translational energies are taken from threshold to 25 eV, initial vibrational states are selected from the lowest few states, and rotational distributions are characterized by temperatures from 0 to 1000 K.

The impact-parameter (IP) method for diatomic molecules as presented by Hazi[11,12] is designed to treat optically allowed transitions. In the preceding paper[13] (paper I) the present authors extended the IP method to treat excitation of vibrationally and rotationally excited initial electronic states to either dissociative or bound energy levels of the final electronic states. The IP method has been shown to give reliable estimates of integral cross sections for high-energy collisions which are comparable to those obtained from the Born approximation and other "plane-wave" methods,[8,14–23] and it agrees well with theoretical methods which are not based upon plane-wave approximations.[11,13] Although the assumptions of the IP model may often not be valid at low energies, it can still provide qualitative information about the effects of vibrational and rotational energy on the cross sections in this region.

The impact-parameter method is described in detail in paper I. Section II of this paper describes the data input into the IP calculations. RKR (Rydberg-Klein-Rees[24]) and *ab initio* electronic structure data are combined and fitted to obtain the best possible potential curves. The dipole transition matrix elements are obtained from *ab initio* calculations. The Born calculations used to calibrate the IP calculations are also presented in Sec. II. In Sec. III the results of the dynamical calculations are presented. Section IV discusses the results and Sec. V summarizes the study.

II. INPUT DATA

A. Potential-energy curves and dipole transition matrix elements

All potential-energy curves and transition dipole moments are fitted as described in paper I: the potential is fitted to the available experimental and/or *ab initio* data points by a cubic spline function and represented at smaller R values by the functional form

$$V(R)=AR^{-1}\exp(-BR)\,, \tag{1}$$

where the parameters are determined by requiring that

Eq. (1) reproduce the two innermost data points. For R values larger than the spline-fit region, the potential has the functional form

$$V(R)=V_0-C_6R^{-6}-C_8R^{-8}, \quad (2)$$

where V_0 is the experimental dissociation energy and the parameters are determined by requiring Eq. (2) to reproduce the outermost potential data points. The cubic spline function is fitted so that the first derivatives at the left and right ends of the spline-fit range match the derivatives of the functional forms of Eqs. (1) and (2), respectively.

Over the range of internuclear distances for which dipole transition moments are available, $M_{\alpha_i\alpha_f}(R)$ is fitted by fourth-order Lagrange interpolation. For smaller values of R, the dipole transition moment is assumed to be constant and equal to the value at the smallest R value for which data is available. For all of the transitions considered here, the dipole transition moments vanish asymptotically. $M_{\alpha_i\alpha_f}(R)$ is extended to large R values by fitting the functional form

$$M_{\alpha_i\alpha_f}(R)=C\exp(-DR) \quad (3)$$

to reproduce $M_{\alpha_i\alpha_f}(R)$ at the two largest R values in the interpolated region. Subroutines for generating the transition dipole moments and potentials used in this work are available from the authors.

1. O_2

Transitions were considered from the ground electronic state of O_2 ($X\,^3\Sigma_g^-$) to three electronic states: the two lowest states of $^3\Sigma_u^-$ symmetry (labeled B and E) and the lowest state of $^3\Pi_u$ symmetry. The potential curves for these states are illustrated in Fig. 1.

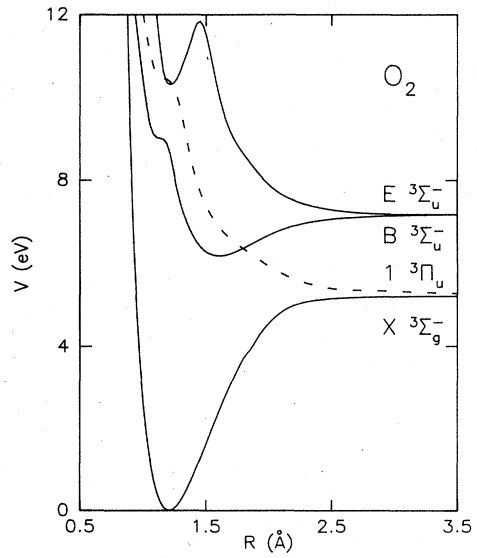

FIG. 1. Potential-energy curves for selected electronic states of O_2. The fits of the curves are described in Sec. II A 1.

For the X state, the RKR data compiled by Krupenie[1] was used in the region from 0.9761 to 1.7915 Å and the results of Saxon and Liu[25] were used from 1.852 to 5.292 Å. The Saxon-Liu results were shifted to have the experimental asymptotic value at 10.584 Å.

The RKR data for the B state[1] were used for values of the internuclear separation between 1.335 15 and 2.575 57 Å. The results of Saxon and Liu[25] were used from 2.646 to 5.292 Å. The *ab initio* points were shifted to have the experimental asymptotic value at 10.584 Å. From 0.953 to 1.270 Å, the results of Redmon and Diffenderfer[26] were used. The points were adjusted to match the interpolated RKR data at 1.376 Å.

No RKR data are available for the $^3\Pi_u$ and E states so the fits were to *ab initio* data. For the $^3\Pi_u$ state, the data points at 0.953 Å and at 1.376—2.646 Å were taken from Ref. 26 and the points in the range 0.995—1.312 Å were taken from Buenker and Peyerimhoff.[27,28] The *ab initio* points were shifted to match the experimental asymptote and to fit smoothly from 1.312 to 1.376 Å.

For the E state, the data points of Ref. 26 were used in the range from 0.953 to 3.175 Å and the results of Saxon and Liu[25] were used from 3.440 to 5.292 Å. The *ab initio* points were shifted to match the experimental asymptote at 10.584 Å and to match each other at 3.175 Å.

All three excited-state curves exhibit either a shoulder or a local well in the potential-energy curves between 1.111 and 1.164 Å. These features are the result of avoided crossings, where the electronic wave function changes character. For example, the B-state wave function changes from a state of Rydberg character to the left of the shoulder to one of valence character to the right of the shoulder.

The transiton dipole moments used in the cross-section calculations are plotted in Fig. 2. These are all fits to the *ab initio* results of Ref. 26, which are similar to those of Ref. 28. For the X-to-B and X-to-$^3\Pi_u$ transitions, the *ab initio* data were available from 0.953 to 2.646 Å; for the X-to-E transition the *ab initio* data were available from 1.111 to 2.249 Å. The dipole transition moment changes rapidly with increasing internuclear distance in the region of the avoided crossing. This type of behavior is not unexpected since the electronic wave function changes character rapidly in this region.

2. S_2

The S_2 molecule is isoelectronic to O_2, so the same transitions were considered: from the ground electronic state $X\,^3\Sigma_g^-$ to the two lowest states of $^3\Sigma_u^-$ symmetry (B and 2) and the lowest state of $^3\Pi_u$ symmetry (B''). The potential curves for these states are illustrated in Fig. 3.

For the X state, the RKR data of Brabson and Volkmar[29] were used in the range from 1.5870 to 2.5456 Å. The RKR data[29] for the B state were used in the range from 1.8093 to 3.0554 Å, and the *ab initio* results of Ref. 26 were used in the range from 1.640 to 1.799 Å. The *ab initio* points were shifted to match an extrapolation of the RKR data at 1.799 Å. The $2\,^3\Sigma_u^-$ and $B''\,^3\Pi_u$ states used the results of Ref. 26 in the range from 1.588 to 3.969 Å.

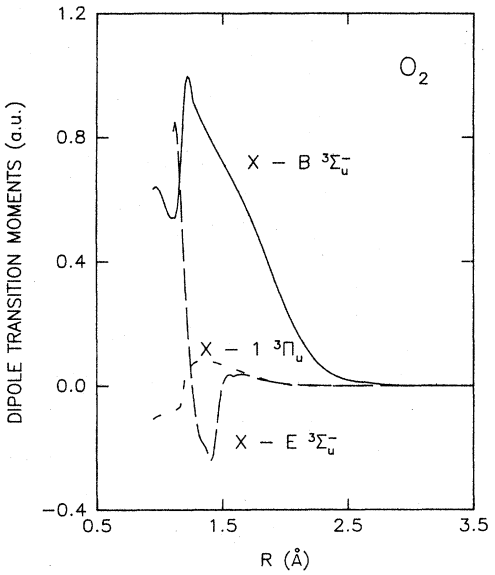

FIG. 2. Dipole transition moments in atomic units as a function of internuclear distance R for transitions from the $X\,^3\Sigma_g^-$ state of O_2 to the $B\,^3\Sigma_u^-$ state (solid line), to the $E\,^3\Sigma_u^-$ state (long-dashed line), and to the $1\,^3\Pi_u$ state (short-dashed line). The curves are interpolations of *ab initio* data as described in Sec. II A 1. (An atomic unit of dipole moment is equal to 2.541 77 Debye.)

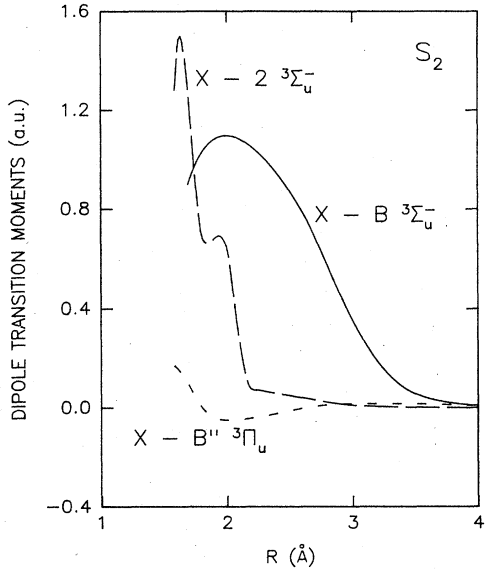

FIG. 4. Dipole transition moments in atomic units as a function of internuclear distance R for transitions from the $X\,^3\Sigma_g^-$ state of S_2 to the $B\,^3\Sigma_u^-$ state (solid line), to the $2\,^3\Sigma_u^-$ state (long-dashed line), and to the $B''\,^3\Pi_u$ state (short-dashed line). The curves are interpolations of *ab initio* data as described in Sec. II A 2. (An atomic unit of dipole moment is equal to 2.541 77 Debye.)

The results for the $2\,^3\Sigma_u^-$ were shifted to reproduce the experimental dissociation energy asymptotically and the B''-state results were shifted to reproduce the experimental dissociation energy at 3.969 Å.

No evidence of avoided crossings in the B and B'' states was found in the region of the potential below 10 eV, but the $2\,^3\Sigma_u^-$ state exhibits a local well above the dissociation limit much like the E state of O_2. The equilibrium geometries of the B and X states of S_2 are more-nearly equal than those of O_2, so the energy of the S_2 B state at the X-state equilibrium geometry lies below the B-state dissociation limit.

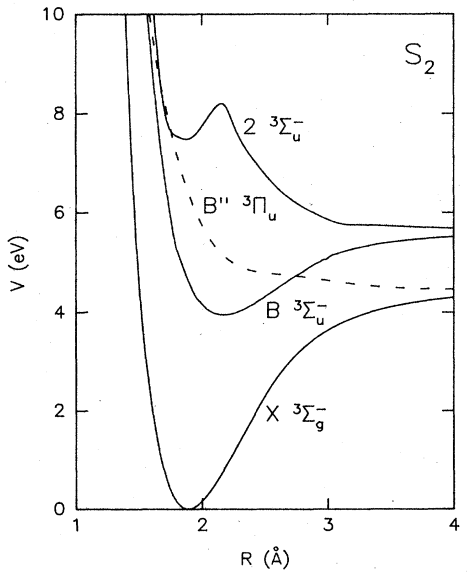

FIG. 3. Potential-energy curves for selected electronic states of S_2. The fits of the curves are described in Sec. II A 2. The zero of energy is the minimum of the ground electronic state.

The transition dipole moments used in the cross-section calculations are plotted in Fig. 4. All were fits to the *ab initio* results of Ref. 26. For the X-to-B transition, *ab initio* data were available from 1.693 to 3.969 Å; for the X-to-B'' transition, the data extended from 1.588 to 3.969 Å; and for the X-to-$2\,^3\Sigma_u^-$ transition, the data extended from 1.588 to 2.910 Å.

B. Minimum impact parameter

In the impact-parameter method, a nonzero b_0 is used as the lower limit in the integration of the transition probability over initial impact parameter to prevent divergence of the cross section.[11,13] The minimum impact parameter is determined by requiring that the results of the impact-parameter method agree with those of the Born approximation (BA) at higher energies (800 eV in the present application). For comparison of the BA and IP results at very high energies the following approximations are made: rotational and vibrational states are treated as being degenerate and the Franck-Condon approximation is assumed to be valid. Within these approximations, the cross sections calculated are for purely electronic transitions summed over all final vibrational and dissociative states, and the IP method reduces to the method as origi-

TABLE I. Minimum impact parameters and transition energies.

	Transition	b_0 (Å)	$\Delta E_{\alpha_i\alpha_f}$ (eV)
O_2	$X \rightarrow B\,^3\Sigma_u^-$	0.921	8.741
	$X \rightarrow E\,^3\Sigma_u^-$	0.138	10.315
	$X \rightarrow 1\,^3\Pi_u$	0.247	10.403
S_2	$X \rightarrow B\,^3\Sigma_u^-$	0.974	4.700
	$X \rightarrow 2\,^3\Sigma_u^-$	2.424	7.480
	$X \rightarrow B''\,^3\Pi_u$	2.28×10^{-16}	6.429

nally formulated by Hazi.[11] At sufficiently high energy the IP cross sections become

$$\sigma^{\alpha_i\alpha_f}(E) \simeq -\frac{2\pi f_{\alpha_i\alpha_f}}{E\,|\,\Delta E_{\alpha_i\alpha_f}\,|}\ln\left[\frac{b_0\,|\,\Delta E_{\alpha_i\alpha_f}\,|}{(2E)^{1/2}}\right], \quad (4)$$

where $\Delta E_{\alpha_i\alpha_f}$ is the transition energy between electronic states, E is the electron translational energy, and $f_{\alpha_i\alpha_f}$ is the electronic oscillator strength, which is related to the dipole transition moment by

$$f_{\alpha_i\alpha_f} = \frac{2m}{3\hbar^2 e^2}\,|\,\Delta E_{\alpha_i\alpha_f}\,|\sum_{\Lambda_i,\Lambda_f}\frac{|\,M_{\alpha_i\alpha_f}(R_e)\,|^2}{g_i}. \quad (5)$$

The sum is over projections of the initial and final electronic angular momentum along the body-fixed axis, m and e are the mass and charge of the electron, $\hbar$ is Planck's constant, and g_i is the degeneracy of the initial electronic state. In the Franck-Condon approximation $M_{\alpha_i\alpha_f}(R)$ is assumed to be a slowly varying function of R and is evaluated at a fixed R value, the equilibrium geometry R_e of the ground electronic state in this case. For a given transition at a fixed translational energy E, $f_{\alpha_i\alpha_f}$ and $\Delta E_{\alpha_i\alpha_f}$ are known and the right-hand side of Eq. (4) is equated to the calculated BA cross section and solved to obtain b_0.

The input required for the Born-approximation calculations consists of the transition energy $\Delta E_{\alpha_i\alpha_f}$, the atomic basis functions, the transformation matrix for constructing the molecular orbitals, and the transition density matrix. The details of the Born calculations are as described by McCurdy and McKoy.[21] The transition energy is obtained from the fits to the potential curves and is the vertical transition energy at R_e, and the electronic structure information is obtained from multiconfiguration self-consistent-field (MCSCF) calculations.[26] The minimum impact parameters obtained from these calculations are presented in Table I along with the transition energies $\Delta E_{\alpha_i\alpha_f}$. All b_0's were evaluated at $E=800$ eV. For O_2, all were evaluated at $R_e=1.207$ Å and for S_2, values of b_0 were evaluated at $R_e=1.889$ Å.

III. RESULTS

First, the vibrational dependence of the electron-impact cross sections was examined. In these calculations the rotational levels were assumed to be degenerate and the cross sections for excitations to bound and dissociative states were calculated from Eqs. (31) and (40) of paper I,[13] respectively. These equations represent the IPV (bound→bound) and IPVD (bound→dissociative) extensions to the original IP method.[11] The effect of rotational excitation is discussed in Sec. III C.

A. O_2

Excitation to the $B\,^3\Sigma_u^-$ state of O_2 is predominantly dissociative. Figures 5 and 6 present the cross sections for excitation to bound states and the dissociative continuum, respectively. Dissociation is favored for this state because its potential in the region of the ground-state equilibrium geometry is repulsive and the overlap of the resultant continuum wave function with the ground-state vibrational wave function is better than its overlap with the bound vibrational energy levels of the excited electronic state. As the initial vibrational energy is increased, the vibrational wave function becomes more diffuse and its overlap with the bound-state wave functions of the excited electronic state improves, causing a large enhancement in this cross section. Near threshold, the dissociative cross sections also increase with increasing initial vibrational energy, mainly because the energetic threshold is decreased as v_i is increased. However, they gradually decrease with increasing initial vibrational energy for higher energies. The IP results for $v_i=0$ agree well with those computed by Chung and Lin[8] using the Born-Ochkur approximation and with the experimental results of Wakiya.[7]

The cross sections for dissociation through the lowest $^3\Pi_u$ state are shown in Fig. 7. These cross sections are typically 20 to 30 times smaller than those for dissociation through the B, state, largely because of the smaller transition dipole matrix elements (see Fig. 2).

The interpretation of the cross sections for excitation to the second excited $^3\Sigma_u^+$ state (the E state) is complicated by the local well in the potential-energy curve above the

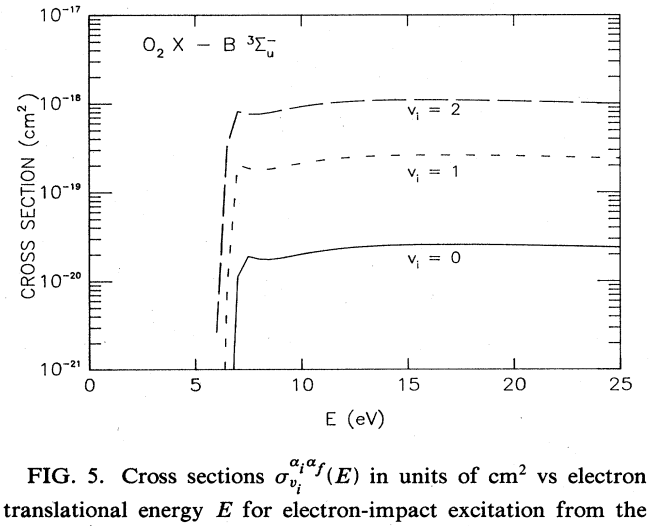

FIG. 5. Cross sections $\sigma_{v_i}^{\alpha_i\alpha_f}(E)$ in units of cm^2 vs electron translational energy E for electron-impact excitation from the ground electronic state of O_2 to bound vibrational states of the B state. The solid, short-dashed, and long-dashed curves are for initial vibrational states $v_i=0$, 1, and 2, respectively.

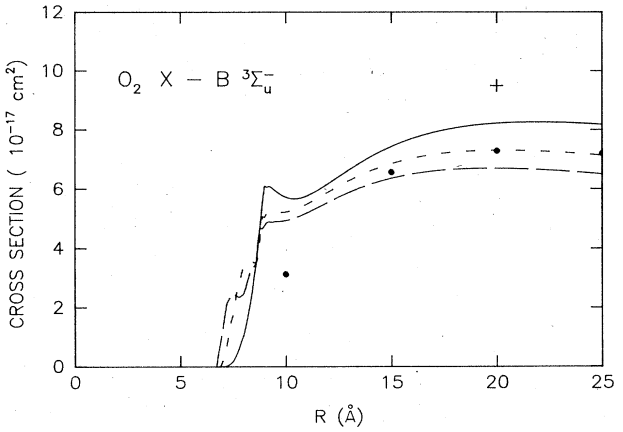

FIG. 6. Cross sections $\sigma_{v_i}^{\alpha_i\alpha_f}(E)$ multiplied by a factor of 10^{17} in units of cm^2 vs electron translational energy E for electron-impact dissociation from the ground electronic state of O_2 through the B state. The solid, short-dashed, and long-dashed curves are for initial vibrational states $v_i=0$, 1, and 2, respectively. The dots are the Born-Ochkur results of Chung and Lin (Ref. 8) and correspond to $v_i=0$. The plus sign is Wakiya's experimental cross section for dissociation from the $v_i=0$ state (Ref. 7).

dissociation limit (see Fig. 1). The potential barrier is 1.5 eV above the local minimum, and the well supports six quasibound states, which will appear as resonances in the elastic cross section for collision of two O atoms. We have performed stabilization[30] calculations to determine the locations of the quasibound states of this potential. Because this local well in the E state lies almost directly above the equilibrium geometry of the X state, there is a large overlap between the vibrational wave functions of the ground state and the quasibound states. Therefore, most of the transitions from the X state go to these quasibound states of the E electronic curve, and there will be very little direct dissociation. However, dissociation from these quasibound states can occur by tunneling. The contribution of these quasibound states to the dissociation cross section is determined by the competition between radiative relaxation to the X state and tunneling predissociation.

The radiative lifetimes of these states have been obtained from the Einstein A factors and are calculated to be on the order of 10^{-10} s. The predissociation tunneling lifetimes can be obtained from the resonance linewidths, which are, in turn, estimated from the Gamow formula.[31] The predissociation tunneling lifetimes are calculated to range from 0.04 s for the lowest quasibound state to 10^{-7} s for the third quasibound state. Thus radiative deexcitation will be the predominant process for the three lowest quasibound states, and they will not contribute to the dissociation cross section.

The cross sections for excitation to these quasibound vibrational states of the E state are presented in Fig. 8. The resonances that occur because of the three upper quasibound states are much broader (i.e., the linewidths are larger and the predissociation lifetimes are of the magnitude or shorter than the radiative lifetime) so they should contribute to the dissociation cross sections. Therefore contributions for final energies above the first three quasibound states were included in the calculations of the dissociation cross sections shown in Fig. 9. The experimental cross section of Wakiya[7] for excitation to bound electronic states in the energy range from 9.7 to 12.1 eV from $v_i=0$ is also shown. The state or states responsible for the transition in this energy range is not definitely known,

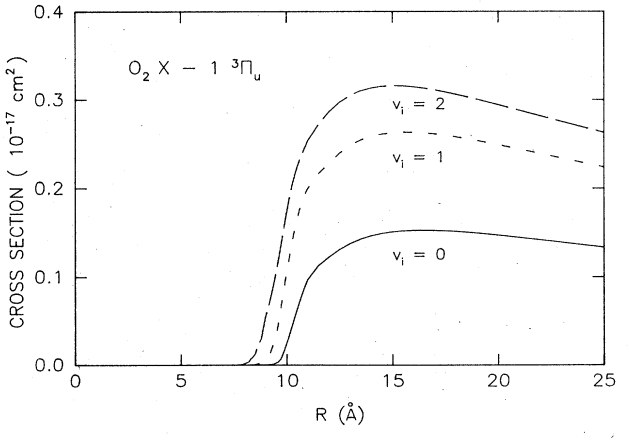

FIG. 7. Cross sections $\sigma_{v_i}^{\alpha_i\alpha_f}(E)$ multiplied by a factor of 10^{17} in units of cm^2 vs electron translational energy E for electron-impact dissociation from the ground electronic state of O_2 through the $1\,^3\Pi_u$ state. The solid, short-dashed, and long-dashed curves are for initial vibrational states $v_i=0$, 1, and 2, respectively.

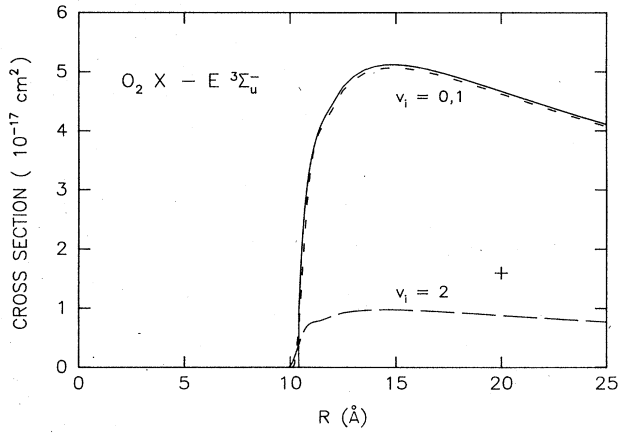

FIG. 8. Cross sections $\sigma_{v_i}^{\alpha_i\alpha_f}(E)$ multiplied by a factor of 10^{17} in units of cm^2 vs electron translational energy E for electron-impact excitation from the ground electronic state of O_2 to quasibound vibrational states of the E state. The solid, short-dashed, and long-dashed curves are for initial vibrational states $v_i=0$, 1, and 2, respectively. The plus sign is Wakiya's experimental cross section for excitation to bound electronic states in the energy region from 9.7 to 12.1 eV (Ref. 7). It is believed to be dominated by optically allowed transitions, especially to the $E\,^3\Sigma_u^-$ state (see Ref. 7).

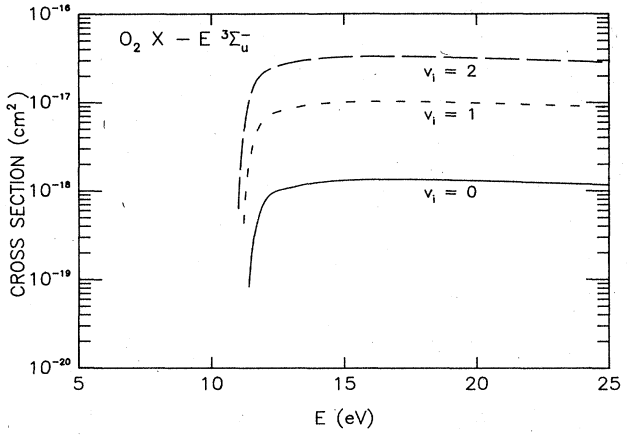

FIG. 9. Cross sections $\sigma_{v_i}^{\alpha_i\alpha_f}(E)$ in units of cm^2 vs electron translational energy E for electron-impact dissociation from the ground electronic state of O_2 through the E state. The solid, short-dashed, and long-dashed curves are for initial vibrational states $v_i=0$, 1, and 2, respectively.

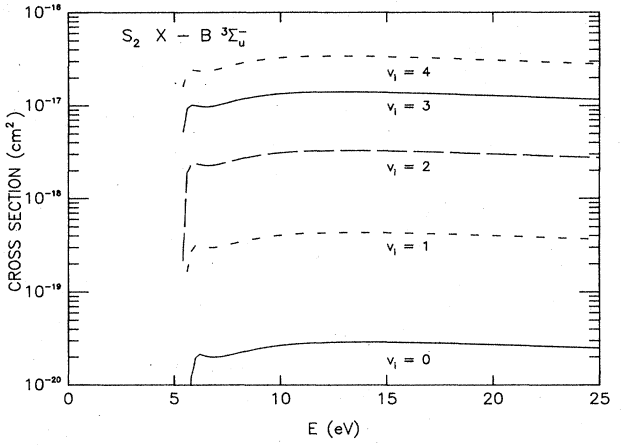

FIG. 11. Cross sections $\sigma_{v_i}^{\alpha_i\alpha_f}(E)$ in units of cm^2 vs electron translational energy E for electron-impact dissociation from the ground electronic state of S_2 through the B state from initial vibrational states $v_i=0$–4. The cross sections are monotonically increasing functions of v_i at all energies.

but it has been suggested that the E state contributes a significant amount to this cross section. The experimental cross section is about 2.5 times lower than the IP results. The discrepancies may be the result of a breakdown in the IP method.

The cross sections for bound-state excitation decrease with increasing initial vibrational state while the dissociative cross sections are greatly enhanced. The dissociative cross sections from the ground vibrational level are 10 to 20 times smaller for the E state than those for the B state, but for the $v_i=2$ state they are only smaller by a factor of 2.

B. S_2

In S_2 the B-state potential curve in the region of the equilibrium geometry for the X state lies below the dissociation limit of the B state; therefore, excitation to bound states predominates. The B-state excitation cross sections are shown in Figs. 10 and 11. The cross sections for transitions to bound states are 2 to 3 orders-of-magnitude larger than the dissociation cross sections. Unlike the O_2 X-to-B case, the vibrational dependence of the bound-state cross sections is very weak and the dissociation cross sections are greatly enhanced as v_i is increased. Again,

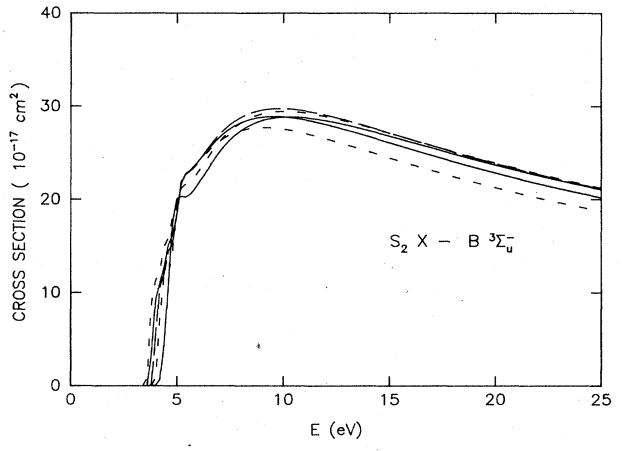

FIG. 10. Cross sections $\sigma_{v_i}^{\alpha_i\alpha_f}(E)$ multiplied by a factor of 10^{17} in units of cm^2 vs electron translational energy E for electron-impact excitation from the ground electronic state of S_2 to bound vibrational states of the B state from initial vibrational states $v_i=0$–4. The solid and short-dashed curves which have the higher threshold energies and are larger at high energy are for $v_i=0$ and 1, respectively. The long-dashed curve is for $v_i=2$ and the other solid and short-dashed curves are for $v_i=3$ and 4, respectively.

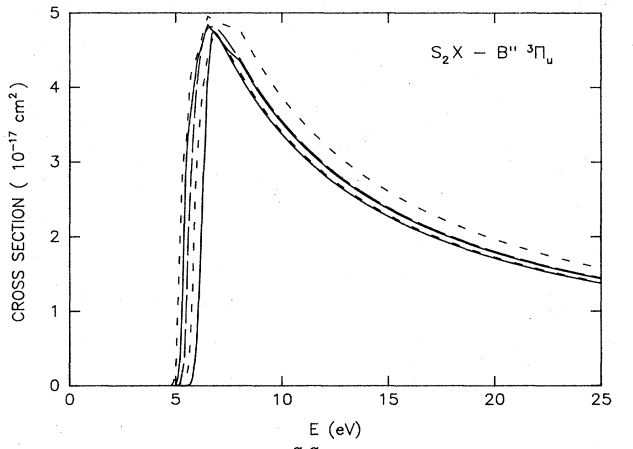

FIG. 12. Cross sections $\sigma_{v_i}^{\alpha_i\alpha_f}(E)$ multiplied by a factor of 10^{17} in units of cm^2 vs electron translational energy E for electron-impact dissociation from the ground electronic state of S_2 through the B'' state from initial vibrational states $v_i=0$–4. The solid and short-dashed curves which have the higher threshold energies and are smaller at high energy are for $v_i=0$ and 1, respectively. The long-dashed curve is for $v_i=2$ and the other solid and short-dashed curves are for $v_i=3$ and 4, respectively.

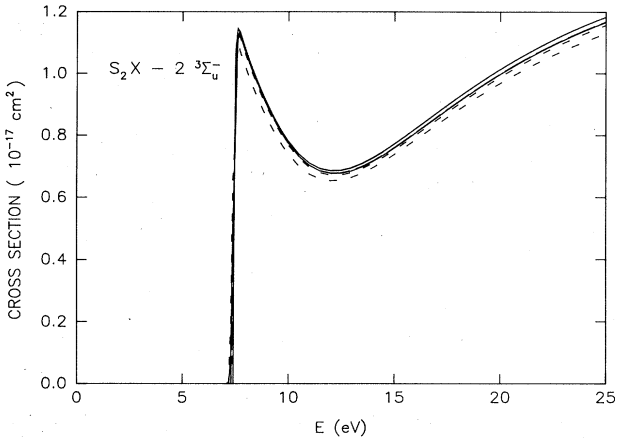

FIG. 13. Cross sections $\sigma_{v_i}^{\alpha_i \alpha_f}(E)$ multiplied by a factor of 10^{17} in units of cm^2 vs electron translational energy E for electron-impact excitation from the ground electronic state of S_2 to quasibound vibrational states of the $2\,^3\Sigma_u^-$ state from initial vibrational states $v_i=0$–4.

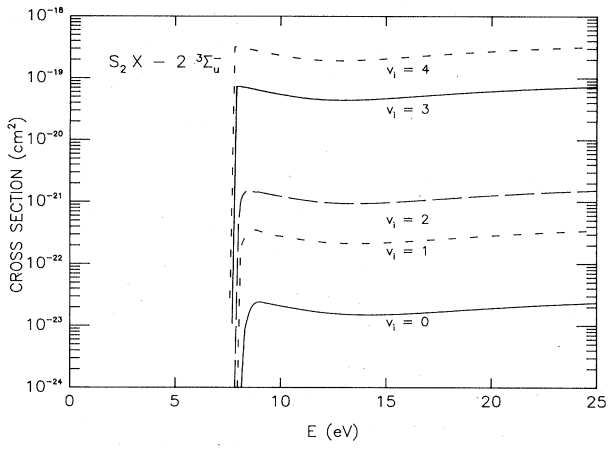

FIG. 14. Cross sections $\sigma_{v_i}^{\alpha_i \alpha_f}(E)$ in units of cm^2 vs electron translational energy E for electron-impact dissociation from the ground electronic state of S_2 through $2\,^3\Sigma_u^-$ state from initial vibrational states $v_i=0$–4. The cross sections are monotonically increasing functions of v_i at all energies. The solid curve which is smaller at high energy is for $v_i=0$. The short-dashed curve which is larger at high energy is for $v_i=1$. The long-dashed curve is for $v_i=2$ and the other solid and short-dashed curves are for $v_i=3$ and 4, respectively.

the smaller cross sections are caused by poor overlap between the initial vibrational wave function and the final wave function for nuclear motion, and larger cross sections result from the wave functions for higher initial vibrational quantum numbers being more diffuse and overlapping better with the final wave function.

The cross sections for dissociation through the B'' state are shown in Fig. 12. These cross sections display only a weak dependence upon initial vibrational state. Compared to the cross sections for the O_2 X-to-1 $^3\Pi_u$ transition, the S_2 cross sections have a much earlier threshold, rise to an earlier peak (only 2 eV above threshold), then decrease more rapidly for higher energies.

Excitation to the $2\,^3\Sigma_u^-$ state of S_2 is very similar to the excitation to the E state of O_2. The $2\,^3\Sigma_u^-$ state has a local well with its minimum almost directly above the X-state minimum; therefore, most of the electron-impact excitation to this state is to the nine quasibound levels of the local well. As for the O_2 E state, the contribution of these quasibound states to the dissociation cross section is determined by the competition between the predissociation tunneling and radiative deexcitation. The lifetimes for predissociation tunneling range from 10^{17} s for $v_f=0$ to 6×10^{-7} s for $v_f=5$. The radiative lifetimes for these states are all approximately 5×10^{-9} s; therefore, excitation to the six lowest quasibound states is considered nondissociative. The cross sections for excitation to the lowest six quasibound states are presented in Fig. 13 and those for dissociation through the $2\,^3\Sigma_u^-$ state are shown in Fig. 14. The dissociative cross sections are more than 4 orders-of-magnitude smaller than the cross sections for excitation to the quasibound states, but they show relatively greater enhancement with increasing v_i.

C. Rotational effects

The effect upon the excitation cross sections of increasing the initial rotational state was investigated for excitations from vibrational levels of the X states of O_2 and S_2.

TABLE II. Cross sections for dissociation of O_2 by electron impact for $v_i=0$.

	E (eV)	$T_{rot}=0$	300	600	1000
X-B	10	5.7(−17)[a]	5.7(−17)	5.7(−17)	5.8(−17)
	15	7.4(−17)	7.5(−17)	7.5(−17)	7.5(−17)
	20	8.2(−17)	8.3(−17)	8.3(−17)	8.3(−17)
X-Π	12	6.2(−19)	6.4(−19)	6.4(−19)	6.4(−19)
	15	7.4(−19)	7.6(−19)	7.7(−19)	7.7(−19)
	20	7.2(−19)	7.4(−19)	7.4(−19)	7.5(−19)
X-E	12	3.9(−19)	7.9(−19)	8.3(−19)	8.4(−19)
	15	8.1(−19)	1.4(−18)	1.4(−18)	1.4(−18)
	20	8.0(−19)	1.3(−18)	1.4(−18)	1.4(−18)

[a]Numbers in parentheses are powers of 10.

TABLE III. Cross sections for dissociation of S_2 by electron impact for $v_i=0$.

	E (eV)	$T_{rot}=0$	300	600	1000
$X\rightarrow B$	6	2.11(−20)[a]	2.07(−20)	2.07(−20)	2.07(−20)
	10	2.82(−20)	2.83(−20)	2.83(−20)	2.85(−20)
	15	3.02(−20)	3.03(−20)	3.03(−20)	3.05(−20)
	20	2.82(−20)	2.82(−20)	2.82(−20)	2.84(−20)
$X\rightarrow\Pi$	6	2.33(−18)	3.26(−18)	3.38(−18)	3.42(−18)
	10	1.69(−17)	1.69(−17)	1.70(−17)	1.70(−17)
	15	1.14(−17)	1.14(−17)	1.14(−17)	1.14(−17)
	20	8.58(−18)	8.63(−18)	8.63(−18)	8.64(−18)

[a]Numbers in parentheses are powers of 10.

The cross sections for bound-to-bound and bound-to-continuum transitions were computed from Eqs. (29) and (38) of paper I, respectively. The method treats the diatomic molecule as a symmetric top, with spin conserved. Thus there are no transitions allowed between multiplet levels. The effect of changing initial rotational states is expected to be much smaller than the effect of increasing the vibrational state. Within the IP method, only transitions in which the rotational quantum number j changes by ±1 are allowed. Therefore increasing j_i does not change the transition energy appreciably, and the threshold energy for excitation changes only slightly. The main effect of increasing j_i is to increase the effective potential by the centrifugal term $j(j+1)/2\mu R^2$. The increase in the potential is larger for smaller R, so the potential well and the vibrational wave function for a given level v_i are shifted to larger internuclear distances and changed in shape slightly. However, changing j_i is a small perturbation on the wave function compared to changing v_i.

Cross sections have been calculated for initial vibrational state $v_i=0$ as a function of translation energy E and rotational temperature T_{rot} for all of the dissociative transitions considered. These are shown in Tables II and III. The cross sections reported in Secs. III A and III B, which assume degeneracy of the rotational states, agree with those computed at $T_{rot}=0$ K using Eqs. (29) and (38) of paper I.[13] Further calculations were performed to test the rotational dependence of $v_i=1$ and 2 and the same quantitative trends were observed.

For O_2 the dissociation cross sections for the X-B and X-Π transitions show very little dependence upon the rotational temperature. However, for the X-E transitions the cross sections increase by almost a factor of 2 as the rotational temperature is increased from 0 to 300 K. This is caused by the centrifugal potential decreasing the bound nature of the E-state potential as j_f is increased and making the effective potential more repulsive, thereby creating better overlap between the initial and continuum wave functions. Since the X-to-E transition contributes very little to the total $v_i=0$ dissociative cross section, no rotational enhancement will be seen; however, for $v_i=2$ the X-to-E transition contributes 30% to 40% of the total dissociation cross section and a slight enhancement will be seen.

The rotational effects are very similar for S_2: the cross sections for both the X-B and X-Π dissociative transitions show very little dependence upon rotational temperature, but the cross section for the X-to-E dissociative transition shows a large enhancement. For S_2 the X-to-2 dissociative cross sections are much smaller than those for the X-to-Π transitions for $v_i=0$—4; however, a large rotational enhancement will be seen for the total dissociation cross sections for these v_i (ranging from a factor of 2 to a factor of 8 for $v_i=0$ and $v_i=4$) as the rotational temperature is increased from 0 to 1000 K.

IV. DISCUSSION

In the IP method it is assumed that the contributions from large impact parameters dominate the cross section. The minimum impact parameter excludes small b where the transition probabilities have unphysical divergent behavior. The extremely small value of b_0 for the X-to-B'' transition in S_2, therefore, reduces the confidence in the reliability of the IP method for this transition at low to intermediate energies.

To estimate the possible contributions to the cross section from small impact parameters, an alternative treatment of the small b region was tested. Instead of assuming the contribution from this region is negligible, the contribution is assumed to be a constant for this range of impact parameters and the cross section is approximated by

$$\tilde{\sigma}^{IP}(E)=\tilde{\sigma}^{IP}_{\tilde{b}_0}+2\pi\int_{\tilde{b}_0}^{\infty} db\, bP^{IP}(b,E)\ , \tag{6}$$

where

$$\tilde{\sigma}^{IP}_{\tilde{b}_0}=\pi\tilde{b}_0^2P(\tilde{b}_0,E)\ . \tag{7}$$

We adjusted $\tilde{b}_0$ to make $\tilde{\sigma}^{IP}(E)$ agree with the BA cross section at 800 eV. A measure of the importance of the region between $b=0$ and $\tilde{b}_0$ is then given by the ratio of $\tilde{\sigma}^{IP}_{\tilde{b}_0}$ to $\tilde{\sigma}^{IP}$. The ratio of $\tilde{\sigma}^{IP}_{\tilde{b}_0}$ to σ^{IP} gives an estimate of the error in $\sigma^{IP}(E)$ due to the treatment of small impact-parameter contributions to the cross section. The value obtained for $\tilde{b}_0$ was generally less than a factor of 2 larger than b_0, and the errors were usually less than 50%.

A source of quantitative errors in the present description of the X-to-B'' transition in S_2 is the potential-energy curve used for the B'' state. The B'' curve of Fig. 3 does have a slight shoulder near 2.5 Å that is not an artifact of the fitting procedure, but previous experimental[32,33] and theoretical[34] evidence indicates that the B'' state should be

slightly bound. Previous (although not definitive) *ab initio* calculations[34] have obtained a minimum in this curve near 2.2 Å at an energy only 0.5 eV below the dissociation limit. In any event, it is very likely that the accessible portion of the B'' potential (near the equilibrium geometry of the X state) does lie above the dissociation limit (of the B'' state) so that electron-impact dissociation will still dominate over excitation to bound states of the well. The shape of the potential will change, thereby changing the quantitative values of the dissociation cross section; most notably the threshold energy should be shifted to lower energies. However, the qualitative predictions that the B'' state will be the major route for electron-impact dissociation will remain the same.

One further complication that arises in both the O_2 and S_2 systems is predissociation by nonadiabatic mechanisms. In O_2 the B state is known to be perturbed by the $1\,^3\Pi_u$ state,[35,36] and, similarly, the S_2 B state is perturbed by the B'' state. In both cases the coupling arises from spin-orbit interactions.[10,33,37,38] The IP method does not account for predissociation by nonadiabatic mechanisms. For the O_2 system, the cross sections for excitation to bound states of the B state are small and predissociation will not contribute significantly to the dissociation cross sections. For S_2 the cross sections for excitation to the bound states are larger than the dissociation cross sections, and predissociation could make a non-negligible contribution to the observed dissociation cross section. Nonadiabatic predissociation could also be important in the $E\,^3\Sigma_u^-$ state of O_2 and the $2\,^3\Sigma_u^-$ state of S_2 since the $1\,^3\Pi_u$ state also crosses these Σ states. However, much less is known about these states (compared to the B states) so it is difficult to estimate the importance of nonadiabatic predissociation for them.

V. SUMMARY

Electron-impact cross sections have been calculated for excitation to bound energy levels of excited electronic states and for dissociation through excited electronic states of O_2 and S_2 using the impact-parameter method. The cross sections were the most strongly influenced by the magnitude of the transition dipole moment and the overlap of the initial vibrational wave function with the final wave function for nuclear motion. The overall dissociation cross sections were often sensitive to the initial vibrational state, but they were nearly independent of the temperature characterizing the thermal distribution of initial rotation states. The major route for electron-impact dissociation of the O_2 ground state at intermediate translational energies (i.e., 5—20 eV above threshold) via dipole-allowed transitions is through the $B\,^3\Sigma_u^-$ state. The X-to-B dissociation cross sections are only weakly dependent upon the initial vibrational state. Although the cross section for the X-to-$^3\Pi_u$ transition does show significant enhancement with increasing v_i, its contribution to dissociation is small; therefore, the total dissociation cross sections show little dependence upon initial vibrational state.

The major dipole-allowed contribution to the cross section for electron-impact dissociation of the S_2 ground vibrational level of the X state comes from transitions to the $B''\,^3\Pi_u$ state. The B''-state cross sections are only slightly enhanced with increasing v_i, but the cross sections for dissociation through the $B\,^3\Sigma_u^-$ state increase significantly and for $v_i=2$ are similar in magnitude to the X-to-B'' dissociation cross sections. Therefore, for S_2, the IP methods predict considerable vibrational enhancement of the overall dissociation cross section.

ACKNOWLEDGMENTS

This research was supported by the Air Force Wright Aeronautical Laboratories, Aero Propulsion Laboratory, Air Force Systems Command, U. S. Air Force, Wright-Patterson Air Force Base, Ohio 43433 under Contract No. F33615-82-C-2241.

*Permanent address: Department of Chemistry, Ohio State University, Columbus, OH 43210.

[1]P. H. Krupenie, J. Phys. Chem. Ref. Data **1**, 423 (1972).
[2]G. M. Lawrence, Phys. Rev. A **2**, 397 (1970).
[3]M. J. Mumma and E. C. Zipf, J. Phys. Chem. **55**, 1661 (1971).
[4]F. Linder and H. Schmidt, Z. Naturforsch. **26a**, 1617 (1971).
[5]S. Trajmar, D. C. Cartwright, and W. Williams, Phys. Rev. A **4**, 1482 (1971).
[6]S. Trajmar, W. Williams, and A. Kuppermann, J. Chem. Phys. **56**, 3759 (1972).
[7]K. Wakiya, J. Phys. B **11**, 3913 (1978); **11**, 3931 (1978).
[8]S. Chung and C. C. Lin, Phys. Rev. A **21**, 1075 (1980).
[9]S. R. Leone and K. G. Kosnik, Appl. Phys. Lett. **30**, 346 (1977).
[10]R. F. Barrow and R. P. duParcq, in *Elemental Sulfur,* edited by B. Meyer (Interscience, New York, 1965).
[11]A. W. Hazi, Phys. Rev. A **23**, 2232 (1981).
[12]A. W. Hazi, T. N. Rescigno, and A. E. Orel, Appl. Phys. Lett. **35**, 477 (1979).
[13]M. J. Redmon, Bruce C. Garrett, L. T. Redmon, and C. W. McCurdy, preceding paper, Phys. Rev. A **32**, 3354 (1985).
[14]S. P. Khare and B. L. Moiseiwitsch, Proc. Phys. Soc. London **88**, 605 (1966).
[15]S. P. Khare, Phys. Rev. **157**, 107 (1967).
[16]K. J. Miller and M. Krauss, J. Chem. Phys. **47**, 3754 (1967).
[17]M. Inokuti, Rev. Mod. Phys. **43**, 297 (1971).
[18]D. C. Cartwright, Phys. Rev. A **2**, 1331 (1970); **5**, 1974 (1972).
[19]S. Chung and C. C. Lin, Phys. Rev. A **6**, 988 (1972); **9**, 1954 (1974).
[20]S. Chung, C. C. Lin, and E. T. P. Lee, Phys. Rev. A **12**, 1340 (1975).
[21]C. W. McCurdy and V. McKoy, J. Chem. Phys. **61**, 2820 (1974).
[22]T. N. Rescigno, C. F. Bender, and V. McKoy, J. Phys. B **8**, L433 (1975).
[23]G. P. Arrighini, F. Biondi, C. Guidotti, A. Biagi, and F. Mar-

inelli, Chem. Phys. **52**, 133 (1980).
[24]R. Rydberg, Z. Phys. **73**, 376 (1931); **80**, 514 (1933); O. Klein, *ibid*. **76**, 226 (1932); A. L. G. Rees, Proc. Phys. Soc. London **59**, 998 (1947).
[25]R. P. Saxon and B. Liu, J. Chem. Phys. **67**, 5432 (1977); **73**, 870 (1980); **73**, 876 (1980).
[26]L. T. Redmon and R. N. Diffenderfer, J. Chem. Phys. (to be published).
[27]R. J. Buenker and S. D. Peyerimhoff, Chem. Phys. Lett. **34**, 225 (1975); Chem. Phys. **8**, 324 (1975).
[28]R. J. Buenker, S. D. Peyerimhoff, and M. Perić, Chem. Phys. Lett. **42**, 383 (1976).
[29]G. D. Brabson and R. L. Volkmar, J. Chem. Phys. **58**, 3209 (1973).
[30]H. S. Taylor, Adv. Chem. Phys. **17**, 91 (1970).
[31]W. H. Miller, J. Phys. Chem. **83**, 960 (1979).
[32]V. E. Bondybey and J. H. English, J. Chem. Phys. **69**, 1865 (1978); **72**, 3113 (1980).
[33]Y. Matsumi, T. Munakata, and T. Kasuya, J. Chem. Phys. **81**, 1108 (1984).
[34]W. C. Swope, Y.-P. Lee, and H. F. Schaefer, III, J. Chem. Phys. **70**, 947 (1979).
[35]P. J. Flory, J. Chem. Phys. **4**, 23 (1936); see also Ref. 16, and references therein.
[36]H. F. Schaefer III and W. H. Miller, J. Chem. Phys. **55**, 4107 (1971).
[37]J. M. Ricks and R. F. Barrow, Can. J. Phys. **47**, 2423 (1969).
[38]M. Heaven, T. A. Miller, and V. E. Bondybey, J. Chem. Phys. **80**, 51 (1984).